Role of N Defects on Thermally Induced Atomic-Scale Structural Changes in Transition-Metal Nitrides

L. Tsetseris,[1,2] N. Kalfagiannis,[1] S. Logothetidis,[1] and S. T. Pantelides[2,3]
[1]Department of Physics, Aristotle University of Thessaloniki, GR-54124 Thessaloniki, Greece
[2]Department of Physics and Astronomy, Vanderbilt University, Nashville, Tennessee 37235, USA
[3]Oak Ridge National Laboratory, Oak Ridge, Tennessee 37831, USA
(Received 2 April 2007; published 19 September 2007)

Transition-metal nitrides (TMN) have exceptional stability, which underlies their use in various applications. Here, we study the role of N point defects on the stability of prototype TMNs using first-principles calculations. We find that distinct regimes for TMN changes relate to specific atomic-scale mechanisms, namely, diffusion of N interstitials (I_N), of I_N pairs, and of N vacancies. The activation of these processes occurs sequentially as the temperature is raised in a range of several hundreds of degrees, accounting for observed TMN changes under widely different conditions.

DOI: 10.1103/PhysRevLett.99.125503 PACS numbers: 61.72.Ji, 68.60.Dv, 72.80.Ga

Transition-metal nitrides (TMN) form a class of compounds which has attracted sustained interest due to their exceptional physical properties [1–5]. Because of their hardness and corrosion resistance, they are used in a variety of applications. For example, TMN films are employed as diffusion barriers [3,4] in microelectronics, and as wear resistant coatings in devices, tools, and bullet proof vests. TiN is regarded as a prototype TMN system, and the structural, mechanical, electronic, and optical properties of bulk [6–8] and nanocrystalline [9] TiN, TiN surfaces [10,11], as well as TiN-based alloys [8,12] and heterostructures [13] have been the focus of several experimental and theoretical studies. TMN-based nanocomposites have emerged recently as candidates for superhard materials [14]. Interest in TiN extends to investigations of the isotopic composition of the sun, as inferred from TiN-based minerals in meteorites [15].

The most common crystalline form of TMNs is the rock salt structure, which is retained for a range of N stoichiometry x. The rock salt TiN phase (δ-TiN), for example, is stable [16,17] for an intriguingly wide range of x ($0.6 \leq x \leq 1.2$), and diffusion barriers and other sought properties can be tailored by selecting specific x values. The importance of point defects arises, therefore, naturally in TMN growth. N vacancies (V_N) and interstitials (I_N), in particular, are regarded as the primary TMN defects. Experimental [8,17–20] and theoretical [8,17,19,21] studies have linked changes in the electronic and mechanical properties of the host crystal to the presence of V_N's. With respect to thermal stability, however, questions on the origin of specific defect-induced changes remain open. Experiments on TiN have identified pertinent activation energies (E_a) of 1.23, 2.09, and 3.9 eV, and similar values have been obtained for other TMNs [1,3,22]. These values point to distinct processes being activated at drastically different temperatures, spanning a range of several hundreds of degrees. And yet, the same mechanisms have been suggested as explanation for different E_a's and different mechanisms have been put forward for the same E_a's. In particular, V_N migration has been suggested for both the E_a's of about 2.1 eV and those of about 3.9 eV [3], while the former value has also been attributed to I_N diffusion [1]. Moreover, the origin of the 1.23 eV value remains an open question, and the 3.9 eV E_a for TiN [22] has been disputed [23], even though E_a's in the same range have been measured for ZrN, UN, and NbN [3]. The resolution of these conflicting suggestions is key for the understanding, control, and optimization of properties of TMN films grown with different techniques and on various substrates.

In this Letter, we use first-principles calculations to elucidate key atomic-scale mechanisms that affect the stability of TiN and ZrN and we resolve the puzzle on the origin of distinct E_a's in TiN. These mechanisms relate to interactions and migration of point defects and they are indeed activated at drastically different temperatures. We first identify the structural properties and interactions among isolated point defects in TiN. We find that the interaction between neighboring V_N's is slightly repulsive and V_N migration has a very high activation energy of 3.8 eV. The lowest energy I_N arrangements are those of split-configurations with stretched N-N bonds aligned along certain crystal directions. In contrast to V_N's, I_N pairs have a substantial binding energy forming complexes in a number of stable configurations. I_N migration is relatively facile and the calculated diffusion barriers (E_d) for isolated I_N's and I_N pairs are 1.3 and 2.0 eV, respectively. We confirm that V_N diffusion is also responsible for the 3.9 eV E_a in the case of ZrN. We finally discuss the stability of Frenkel V_N-I_N pairs. Overall these internally consistent assignments of activation energies provide a systematic account for key observations related to the stability of these materials.

The calculations were performed within density-functional theory (DFT), with a generalized-gradient cor-

rected (GGA) exchange-correlation functional [24], a plane wave basis set with an energy cutoff (E_c) of 400 eV, and projector-augmented wave potentials [25], as implemented in the VASP code [26]. The supercells we used were $2 \times 2 \times 2$, $3 \times 3 \times 3$, $4 \times 4 \times 4$ in terms of the conventional unit cell. The lattice constant was fixed at 4.2366 Å [6,9]. The results we present below are based on the $3 \times 3 \times 3$ supercell with 108 Ti and 108 N atoms when no defects are present. We used a varying number of k points following the Mohnkorst-Pack scheme [27] for Brillouin zone sampling. In particular, we used $2 \times 2 \times 2$ and $3 \times 3 \times 3$ grids for the majority of the results on the above-mentioned large supercells. In the following we report only the $3 \times 3 \times 3$ results, unless stated otherwise. Previous studies [28] showed the importance of k-point sampling for the calculation of TiN elastic constants. In the present case, we find by comparing to calculations with finer grids ($6 \times 6 \times 6$) that the relevant quantities (relative stability of defects, defect binding energies, and barriers) are converged within about 0.1 eV. This accuracy is sufficient to decide on the role of the point defects discussed here on TMN thermal stability. E_d's were calculated with the elastic band (EB) method [29] for minimum energy pathways (MEP), as described in previous studies [30] that obtained DFT-GGA E_a's within 0.1–0.2 eV from the experimental values. The interaction energies E_i between defects were obtained combining the energy of the host crystal and the energies of supercells with isolated defects and with defect complexes.

In agreement with Jhi *et al.* [21], we found that a N vacancy induces a small outward relaxation in the surrounding TiN matrix. The distance between neighboring Ti atoms and the V_N site changes from the pristine 2.12 to 2.20 Å. The backbonds of these Ti atoms to Ti species of the second shell around the vacancy contract from 2.99 to 2.93 Å.

The outward relaxation is obtained only for the converged calculations with the larger $3 \times 3 \times 3$ and $4 \times 4 \times 4$ supercells. The calculation with the smaller $2 \times 2 \times 2$ supercell and Γ-point sampling gives a slight inward relaxation for the Ti atoms around the N vacancy. In Fig. 1(a) we show the transition state (TS) of V_N diffusion. We started with an initial guess for the MEP with the vacancy migrating through the body centered position of the conventional cubic unit cell around the defect. This MEP relaxed with the EB calculation to a path that crosses one of the stretched Ti-Ti bonds around the V_N site, as shown in Fig. 1(a). The diffusion barrier is 3.8 eV, in excellent agreement with one of the reported [22] experimental E_a's. The E_d value is sensitive to the calculational parameters. For an energy cutoff E_c of 300 eV the computed E_d was 3.88 eV, and for Γ-point sampling the value was significantly lower, 3.43 eV. Calculations with an E_c of 400 eV and a $2 \times 2 \times 2$ k grid give an E_a of 3.95 eV. Use of a finer grid ($6 \times 6 \times 6$) for the total energies of configurations obtained with $3 \times 3 \times 3$ sampling gives an E_a of at least 3.76 eV, confirming the convergence of results.

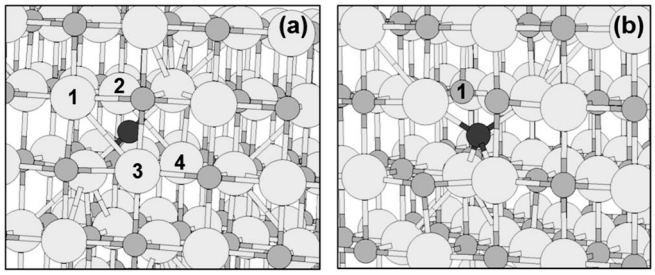

FIG. 1. Transition states for point defect migration in TiN: (a) V_N diffusing ($E_d = 3.8$ eV) between the midpoints of 1–2 and 3–4 Ti-Ti bonds. (b) I_N migration ($E_d = 1.08$ eV) between the split I_N configurations of Fig. 2(a) (I_N bonds to N atom 1) and Fig. 2(c). The diffusion barrier between the lowest energy configurations of Fig. 2(b) is 1.28 eV. (Ti: light gray, N: gray, interstitial N: dark gray spheres.)

The large barrier indicates that V_N diffusion is activated only at very high temperatures. This fact is central in explaining the stability of TiN_x, and for other TMNs, since similar E_a's of 3.4, 3.9, 4.1, and 4.8 eV have been measured for N diffusion in $ZrN_{0.69}$, $ZrN_{0.95}$, UN, and NbN, respectively [3]. The accuracy of the experiments that obtained the 3.9 eV value for TiN, however, has been under debate [1,23]. We, therefore, studied also V_N migration in ZrN. V_N hopping in ZrN follows the same path as V_N's in TiN, with a TS similar to the one shown in Fig. 1(a). The calculated barrier is 3.86 eV ($2 \times 2 \times 2$ k grid), in excellent agreement with the N E_d of 3.9 eV in near stoichiometric ZrN [3]. This agreement corroborates the result of 3.9 eV in TiN, and we therefore infer that V_N diffusion is indeed associated with the reported high E_a's in TMNs.

N vacancies are believed to be the defects that control the stoichiometry of TiN films and their mutual interactions underlie the properties of TiN_x films. We studied the V_N-V_N interactions for 3 N divacancy configurations: (i) both V_N's were placed in the same (110) chain, (ii) the V_N's were neighboring members of a (100) chain, and (iii) the two V_N's were placed in a distance of 7.9 Å with respect to each other. The results are given through the interaction energies (E_i). Positive (negative) E_i's indicate repulsion (attraction) between defects. For the divacancies, E_i's are slightly positive (about 0.15 eV) for neighboring V_N's and they decrease to zero as the two defects move away from each other.

N interstitials is the second class of primary point defects in TMNs. Unlike N vacancies, which appear only in one configuration, a number of possibilities exist for I_N's. One possibility is for an I_N to occupy a tetrahedral position, as shown in Fig. 2(c). Other possible arrangements are split interstitials for which I_N forms a stretched N-N bond of 1.33 Å with a N atom of the network. This stretched bond may be aligned along different directions. In particular, we found two stable configurations with the N-N dimer point-

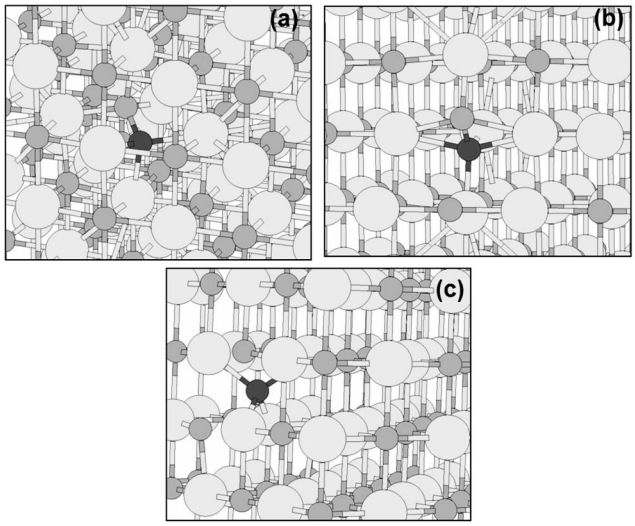

FIG. 2. (a) and (b) split I_N's in TiN with N-N stretched bonds along (111) and (10$\bar{1}$) directions, (c) tetrahedral I_N. Lowest energy I_N configuration is (b). Structures (a) and (c) are 0.20 and 0.86 eV higher in energy, respectively. (Ti: light gray, N: gray, interstitial N: dark gray spheres.)

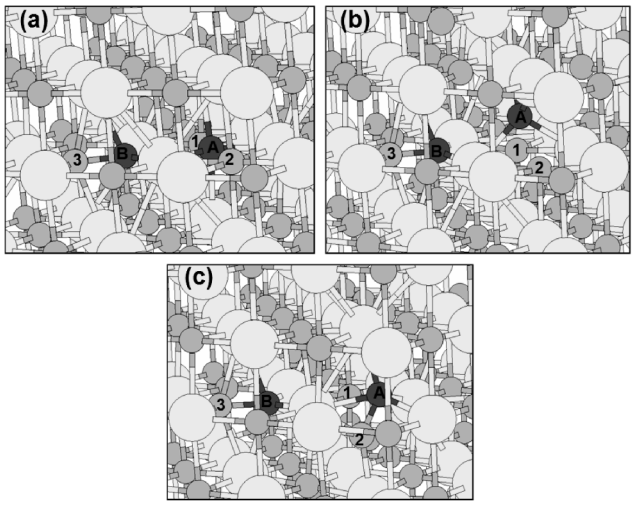

FIG. 3. Pairs of I_N's shown in Fig. 2: (a) vicinal I_N^b-I_N^b pair bound by 0.55 eV, (b) vicinal I_N^b-I_N^c, and (c) two I_N^b's in a second nearest neighbor distance and bound by 0.44 eV. N atoms 3-B form one I_N^b complex. N atom A moves from the 1-A I_N^b in (a), to tetrahedral position in (b), and connects to 2-A I_N^b in (b). The (a)–(c) E_d of 1.97 eV is the diffusion E_a for a I_N-I_N pair in TiN. (Ti: light gray, N: gray, interstitial N: dark gray spheres.)

ing along the (111) and (10$\bar{1}$) directions. They are depicted in Figs. 2(a) and 2(b), respectively. I_N^b is the most stable. I_N^a is higher in energy, by 0.20 eV, and the tetrahedral I_N^c is considerably less stable by 0.86 eV. Diffusion between the lowest energy I_N^b configurations proceeds with hopping through I_N^a and I_N^c. The TS for a migration step between I_N^a and I_N^c is shown in Fig. 1(b). The barrier is 1.08 eV. We also computed the MEP for the transformation between I_N^a and I_N^b configurations at the same site. This latter MEP has a very small barrier, less than 0.2 eV. Combining the results of both MEPs and the relative stability of I_N's, the effective I_N diffusion barrier is 1.28 eV. This relatively low value indicates that I_N migration is activated at dramatically lower temperatures than N vacancies.

In contrast to V_N, the interaction among I_N's can be strongly attractive for a number of configurations. Two neighboring split interstitials, prepared with their N-N stretched bonds aligned in parallel, relax to a herringbone configuration with the N-N bonds perpendicular to each other. The most stable structure is the one with both interstitials in the I_N^b configuration of Fig. 2(b). The binding energy of this I_N^b-I_N^b complex, shown in Fig. 3(a), is considerable and equal to 0.55 eV. When one of the I_N's switches to a vicinal I_N^a or I_N^c configuration the energy increases by 0.14 and 1.33 eV, respectively. The latter I_N^b-I_N^c complex, which is depicted in Fig. 3(b), is encountered as an intermediate configuration during the diffusion of an I_N-I_N pair. A second intermediate structure is shown in Fig. 3(c) with two I_N^b interstitials bound by 0.44 eV in second nearest neighbor distance to each other. The activation energy for the transformation between the structures of Figs. 3(a)–3(c) is 1.97 eV, obtained as the difference between the energies of the I_N^b-I_N^b complex and the TS of the Fig. 3(b) and 3(c) hopping. After one of the I_N's hops so that the complex changes from the initial to the final configuration of Fig. 3, the other I_N atom can perform similar steps. As a result, a migration step for the I_N^b-I_N^b complex can be completed. Therefore, the 1.97 value is the calculated diffusion barrier for the stable I_N-I_N complex in TiN.

Thermal stability depends also on the properties of Frenkel V_N-I_N pairs If there is a path that takes a remote I_N in the immediate vicinity of a V_N and this path does not include sites of high energy, then the mutual annihilation of V_N's and I_N's will be possible when the migration of one of the species is activated. We considered a number of V_N and I_N combinations. We created a V_N at one of the closest to a I_N^a N site (i) on the (110) line, (ii) on the (01$\bar{1}$) line, and (iii) at a remote site in the same supercell. Likewise for I_N^b, we created a V_N (i) at one of the closest to the I_N N site on the same (10$\bar{1}$) line, (ii) at one of the closest to the I_N N site, but on a neighboring (10$\bar{1}$) line, and (iii) at a remote site in the same supercell. All these configurations, save for the ones with large I_N-V_N distances, relax to an ideal TiN network as the I_N moves to the neighboring V_N. The FP configurations (i) and (ii) can be viewed as precursors before the mutual V-I annihilation. Alternatively, they can be viewed as the first intermediate configurations after the FP creation and before its dissociation due to the migration of I_N. Because there is no barrier between these configurations and the ideal crystal, we conclude that I_N migration is the rate-limiting step for the annihilation or creation of FPs.

The results of this work are consistent with three regimes with distinct rate-limiting steps. Depending on

growth conditions, the thermal stability of a TMN film may fall in one particular regime, or a sequence of distinct processes may be encountered as the temperature is raised. It is believed that low-energy ion deposition creates I_N's [3]. In this case, diffusion of isolated I_N's with an E_a of 1.28 eV gives rise to defect-related changes, as excess N annihilates vacancies or gets trapped at surfaces and grain boundaries. The process is consistent with stress relaxation measurements [3] at relatively low ($\approx$200–500 °C) temperatures. Alternatively, growth can lead to the formation of stable I_N pairs. Their calculated diffusion barrier, 1.97 eV, is in very good agreement with a measured [1] E_a of 2.09 eV. Hence, I_N pair migration can account for changes in TMN properties under annealing at higher temperatures ($\approx$500–800 °C). We should note that indirect evidence for I_N migration is offered by the occasional formation of N_2 bubbles in TiN [3]. Finally, an E_a of 3.8 eV, in agreement with experiments at even higher temperatures, is expected when V_N's dominate a sample. Indeed, changes in properties such as color which can be attributed to V migration [18], occur only after prolonged annealing at temperatures above 900 °C.

Our findings have implications also for the stability and properties of TMNs away from the ideal 1:1 stoichiometry. The large V_N diffusion barrier underlies the stability of substoichiometric films. The suppression of V_N migration preserves the rock salt structure, and it is consistent with the random distribution of V_N's, as observed [18]. An overstoichiometric TMN_x film is expected to be less stable in terms of atomic-scale structural changes, because I_N migration is much easier to activate. Let us also note that the selection of a particular substrate can play a decisive role for the thermal stability of TMN films. Changes in the lattice constants away from bulk values can give rise to considerable variations in the activation of the processes discussed above.

Finally, we should stress that other physical mechanisms may also be operative in TMN films, such as the nucleation and migration of extended defects like dislocations, or the formation of microvoids [3]. Other point defects (cation vacancies and interstitials, antisites, etc.), which are generally believed to be less mobile [3] may be present and affect physical properties. A comprehensive account of thermal stability also includes aspects such as phase separation and equilibrium, recrystallization, interfacial reactions, and oxidation [3]. The study of all these aspects, however, is beyond the scope of the present work; here, we have focused on the crucial role of N defects as the primary agents for atomic-scale structural stability. The results on the key processes of N defect migration are in agreement with experimental measurements and they settle long-standing questions on the origin of observed changes during annealing.

We acknowledge support by the McMinn Endowment at Vanderbilt University, AFOSR MURI Grant Nos. FA9550-05-1-0306, and GSRT-ΠΕΝΕΔ-03ΕΔ613. The calculations were performed at ORNL's Center for Computational Sciences.

[1] A. J. Perry, J. Vac. Sci. Technol. A **6**, 2140 (1988), and references therein.
[2] S. H. Jhi *et al.*, Nature (London) **399**, 132 (1999).
[3] L. Hultman, Vacuum **57**, 1 (2000), and references therein.
[4] F. Lévy *et al.*, Surf. Coat. Technol. **120–121**, 284 (1999).
[5] I. Pollini, A. Mosser, and J. C. Parlebas, Phys. Rep. **355**, 1 (2001).
[6] H. Höchst *et al.*, Phys. Rev. B **25**, 7183 (1982).
[7] Z. Dridi *et al.*, J. Phys. Condens. Matter **14**, 10237 (2002).
[8] M. Guemmaz *et al.*, J. Phys. Condens. Matter **9**, 8453 (1997); M. Guemmaz *et al.*, J. Electron Spectrosc. Relat. Phenom. **107**, 91 (2000); M. Guemmaz *et al.*, Int. J. Inorg. Mater. **3**, 1319 (2001).
[9] J. Hu *et al.*, J. Am. Ceram. Soc. **83**, 430 (2000).
[10] P. A. P. Lindberg *et al.*, Phys. Rev. B **36**, 939 (1987).
[11] B. W. Karr *et al.*, Phys. Rev. B **61**, 16137 (2000); S. Kodambaka *et al.*, Surf. Sci. **513**, 468 (2002); C. S. Shin *et al.*, J. Appl. Phys. **95**, 356 (2004).
[12] L. Calmels, C. Mirguet, and Y. Kihn, Phys. Rev. B **73**, 024207 (2006).
[13] P. Patsalas and S. Logothetidis, J. Appl. Phys. **93**, 989 (2003).
[14] S. Hao *et al.*, Phys. Rev. Lett. **97**, 086102 (2006).
[15] A. Meibom *et al.*, Astrophys. J. **656**, L33 (2007).
[16] J. H. Kang and K. J. Kim, J. Appl. Phys. **86**, 346 (1999).
[17] C. S. Shin *et al.*, J. Appl. Phys. **93**, 6025 (2003).
[18] J. P. Schaffer *et al.*, J. Vac. Sci. Technol. A **10**, 193 (1992).
[19] M. Tsujimoto *et al.*, J. Electron Spectrosc. Relat. Phenom. **143**, 159 (2005).
[20] T. Lee *et al.*, Phys. Rev. B **71**, 144106 (2005).
[21] S. H. Jhi *et al.*, Phys. Rev. Lett. **86**, 3348 (2001).
[22] V. S. Eremeev, Y. M. Ivanov, and A. S. Panov, Izv. Akad. Nauk SSSR Met. **5**, 262 (1969).
[23] F. W. Wood and O. G. Paasche, Thin Solid Films **40**, 131 (1977).
[24] J. P. Perdew and Y. Wang, Phys. Rev. B **45**, 13244 (1992).
[25] P. E. Blöchl, Phys. Rev. B **50**, 17953 (1994).
[26] G. Kresse and J. Joubert, Phys. Rev. B **59**, 1758 (1999).
[27] D. J. Chadi, and M. L. Cohen, Phys. Rev. B **8**, 5747 (1973).
[28] S. Nagao, K. Nordlund, and R. Nowak, Phys. Rev. B **73**, 144113 (2006).
[29] G. Mills, H. Jónsson, and G. K. Schenter, Surf. Sci. **324**, 305 (1995).
[30] L. Tsetseris, S. W. Wang, and S. T. Pantelides, Appl. Phys. Lett. **88**, 051916 (2006); L. Tsetseris and S. T. Pantelides, Phys. Rev. Lett. **97**, 116101 (2006).